In summary, this study is the first regarding the potential role of visfatin in the disease process of dcSSc. Visfatin may exert a direct anti-fibrotic effect on dermal fibroblasts and an indirect anti-fibrotic effect by promoting Th1 immune polarization in dcSSc. The present data further support an emerging idea that adipocytokines play an important role in the pathogenesis of autoimmune diseases, including SSc.

Rheumatology key messages

- Serum visfatin levels increase in late-stage dcSSc when skin sclerosis spontaneously regresses.
- Visfatin exerts a direct anti-fibrotic effect on SSc dermal fibroblasts, but not on normal fibroblasts.
- Visfatin-dependent Th1 immune polarization may contribute to regression of skin sclerosis in late-stage dcSSc.

Acknowledgements

We thank Tamami Kaga and Yoshiko Ito for technical help with cell culture.

Funding: This work was supported by a grant for Research on Intractable Diseases from the Ministry of Health, Labour, and Welfare of Japan.

Disclosure statement: The authors have declared no conflicts of interest.

Supplementary data

Supplementary data are available at *Rheumatology* Online.

References

1 Masui Y, Asano Y, Shibata S *et al*. Serum adiponectin levels inversely correlate with the activity of progressive skin sclerosis in patients with diffuse cutaneous systemic sclerosis. J Eur Acad Dermatol Venereol 2012;26:354–60.

2 Fukuhara A, Matsuda M, Nishizawa M *et al*. Visfatin: a protein secreted by visceral fat that mimics the effects of insulin. Science 2005;307:426–30.

3 Moschen AR, Kaser A, Enrich B *et al*. Visfatin, an adipocytokine with proinflammatory and immunomodulating properties. J Immunol 2007;178:1748–58.

4 Huang JF, Huang CF, Yu ML *et al*. Serum visfatin is correlated with disease severity and metabolic syndrome in chronic hepatitis C infection. J Gastroenterol Hepatol 2011;26:530–5.

5 Kukla M, Ciupińska-Kajor M, Kajor M *et al*. Liver visfatin expression in morbidly obese patients with nonalcoholic fatty liver disease undergoing bariatric surgery. Pol J Pathol 2010;61:147–53.

6 Yu XY, Qiao SB, Guan HS *et al*. Effects of visfatin on proliferation and collagen synthesis in rat cardiac fibroblasts. Horm Metab Res 2010;42:507–13.

7 Jia SH, Li Y, Parodo J *et al*. Pre-B cell colony-enhancing factor inhibits neutrophil apoptosis in experimental inflammation and clinical sepsis. J Clin Invest 2004;113:1318–27.

8 Bao JP, Chen WP, Wu LD. Visfatin: a potential therapeutic target for rheumatoid arthritis. J Int Med Res 2009;37:1655–61.

9 Ozgen M, Koca SS, Aksoy K *et al*. Visfatin levels and intima-media thicknesses in rheumatic diseases. Clin Rheumatol 2011;30:757–63.

10 LeRoy EC, Black C, Fleischmajer R *et al*. Scleroderma (systemic sclerosis): classification, subsets and pathogenesis. J Rheumatol 1988;15:202–5.

11 Preliminary criteria for the classification of systemic sclerosis (scleroderma). Subcommittee for scleroderma criteria of the American Rheumatism Association Diagnostic and Therapeutic Criteria Committee. Arthritis Rheum 1980;23:581–90.

12 Asano Y, Stawski L, Hant F *et al*. Endothelial Fli1 deficiency impairs vascular homeostasis: a role in scleroderma vasculopathy. Am J Pathol 2010;176:1983–98.

13 Takeda K, Hatamochi A, Ueki H *et al*. Decreased collagenase expression in cultured systemic sclerosis fibroblasts. J Invest Dermatol 1994;103:359–63.

14 Kuroda K, Shinkai H. Gene expression of types I and III collagen, decorin, matrix metalloproteinases and tissue inhibitors of metalloproteinases in skin fibroblasts from patients with systemic sclerosis. Arch Dermatol Res 1997;289:567–72.

15 Matsushita T, Hasegawa M, Hamaguchi Y *et al*. Longitudinal analysis of serum cytokine concentrations in systemic sclerosis: association of interleukin 12 elevation with spontaneous regression of skin sclerosis. J Rheumatol 2006;33:275–84.

16 Otero M, Lago R, Gomez R *et al*. Changes in plasma levels of fat-derived hormones adiponectin, leptin, resistin and visfatin in patients with rheumatoid arthritis. Ann Rheum Dis 2006;65:1198–201.

17 Brentano F, Schorr O, Ospelt C *et al*. Pre-B cell colony-enhancing factor/visfatin, a new marker of inflammation in rheumatoid arthritis with proinflammatory and matrix-degrading activities. Arthritis Rheum 2007;56:2829–39.

18 Nowell MA, Richards PJ, Fielding CA *et al*. Regulation of pre-B cell colony-enhancing factor by STAT-3-dependent interleukin-6 trans-signaling: implications in the pathogenesis of rheumatoid arthritis. Arthritis Rheum 2006;54:2084–95.

19 Busso N, Karababa M, Nobile M *et al*. Pharmacological inhibition of nicotinamide phosphoribosyltransferase/visfatin enzymatic activity identifies a new inflammatory pathway linked to NAD. PLoS One 2008;3:e2267.

20 Yuan C, Liang NL, Liu XJ *et al*. [Effect of visfatin on the expression of basic fibroblast growth factor in rat hepatic stellate cells]. Sichuan Da Xue Xue Bao Yi Xue Ban 2010;41:617–20.

Clinical Immunology (2013) 147, 71–78

available at www.sciencedirect.com

Clinical Immunology

www.elsevier.com/locate/yclim

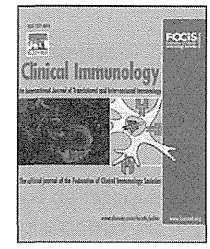

Ghrelin attenuates collagen production in lesional fibroblasts from patients with systemic sclerosis☆

Yuko Ota, Yasushi Kawaguchi*, Kae Takagi, Hisae Ichida, Takahisa Gono, Masanori Hanaoka, Tomoaki Higuchi, Hisashi Yamanaka

Institute of Rheumatology, Tokyo Women's Medical University, 10-22 Kawada-cho, Shinjuku-ku, Tokyo 162-0054 Japan

Received 10 January 2013; accepted with revision 5 March 2013
Available online 13 March 2013

KEYWORDS
Ghrelin;
Systemic sclerosis;
Fibrosis;
Interstitial lung disease

Abstract Systemic sclerosis (SSc) is a connective tissue disease characterized by thickening of the skin and tissue fibrosis of the internal organs. Ghrelin is primarily described as a gut hormone, and many studies currently indicate that ghrelin has protective effects in different organs, including the heart, pancreas, lung and liver, resulting from its anti-fibrotic properties. We found decreased levels of ghrelin in the plasma from patients with SSc compared with those from healthy controls. In skin fibroblast cultures, recombinant ghrelin diminished the production of collagen type I. In addition, the mRNA levels of *COL1A2* and *TGFB* genes were significantly decreased by the stimulation of ghrelin. We showed that ghrelin may exert anti-fibrotic effects in the skin fibroblasts from patients with SSc. Because the plasma levels of ghrelin are low in SSc, the administration of ghrelin could be a new strategy for the treatment of SSc.

1. Introduction

Systemic sclerosis (SSc) is a multisystem disorder of connective tissue characterized by the excessive accumulation of extracellular matrix in the skin and various internal organs [1,2]. Although the pathogenesis of SSc is not fully understood, autoimmunity may be involved because the production of SSc-specific autoantibodies has been well established for the past two decades, including anti-topoisomerase I antibody, anti-centromere antibody, and anti-RNA polymerase I/III antibody [3]. Fibrosis and endothelial injury are the central manifestations of SSc [4]. Skin fibrosis, interstitial lung disease, gastrointestinal involvement, and cardiac involvement may result from the fibrosis [5]. The pathological examinations of the tissue fibrosis revealed the abnormality of extracellular matrix production in the lesional tissues of patients with SSc [6]. More than 90% of patients with SSc develop gastrointestinal tract involvement [7], but severe manifestations such as pseudo-obstruction, severe constipation, megacolon and malabsorption syndrome are rarely observed in patients with SSc. Although intestinal involvement is believed to result from smooth muscle fibrosis [8], the pathophysiology of the intestinal involvement is not fully understood. Unfortunately, intestinal involvement is often detected when severe complications have already occurred, and it is irreversible and difficult to manage [9]. Therefore, finding new treatments for the organ fibrosis associated with SSc is extremely important.

☆ This work is supported by systemic sclerosis and mixed connective tissue disease research grants from the Ministry of Health, Labour and Welfare, Japan.
* Corresponding author. Fax: +81 3 5269 1726.
E-mail address: y-kawa@ior.twmu.ac.jp (Y. Kawaguchi).

1521-6616/$ - see front matter © 2013 Elsevier Inc. All rights reserved.
http://dx.doi.org/10.1016/j.clim.2013.03.001

Ghrelin, a 28-amino-acid peptide with n-octanoylation indispensable for binding to the growth hormone secretagogue receptor (GHSR), was originally discovered in human and rat stomachs in 1999 [10]. Ghrelin molecules are present as two major endogenous forms, an acylated ghrelin and a desacylated ghrelin [11]. The modification is highly susceptible to circulating esterases, which can convert the active form of ghrelin (acylated form) to the desacylated form [12]. This conversion can occur within minutes after sample collection and can lead to variability and distracting artifacts in acylated ghrelin measurements. In addition to potent growth hormone-releasing effects, ghrelin has been found to have other peripheral effects. Although ghrelin mRNA is particular abundant in the stomach and intestine, it is also expressed at low levels in other organs, notably, the brain, pituitary gland, heart, lung, pancreas, kidney, and placenta [13]. One of the most important biological activities of ghrelin is the stimulation of food intake during the long-term regulation of body weight [14]. The wide distribution of the GHSR in various organs suggests a potentially broad array of actions for ghrelin. Recently, in addition to growth hormone-releasing effects, peripheral effects such as cytoprotection, vasodilatation, and anti-inflammation have been attributed to ghrelin [15,16].

Plasma ghrelin levels increase upon fasting and insulin-induced hypoglycemia and decrease in response to the oral or intravenous administration of glucose. The fasting plasma ghrelin level is elevated in anorexia nervosa and cachexia and is reduced in obesity [17,18]. In autoimmune diseases, the serum ghrelin levels have been measured in patients with rheumatoid arthritis and ANCA-associated vasculitis [19,20]. In patients with rheumatoid arthritis, the serum ghrelin levels did not differ from those of the healthy group. Conversely, the serum ghrelin levels were significantly elevated in patients with ANCA-associated vasculitis compared with the healthy controls (HCs), and the levels were correlated with disease activity.

In 2008, rikkunshito, an herbal medicine, was shown to suppress cisplatin-induced anorexia in rats by increasing the plasma acylated ghrelin. Recent studies also indicated that recombinant ghrelin was successfully administered to patients with a variety of disorders, such as anorexia, caquexia, and gastroparesis [21]. Moreover, ghrelin improves the functional capacity in elderly patients with congestive heart failure and chronic obstructive pulmonary disease, which might be due to its anti-fibrotic effects.

The aim of this study was to investigate the levels of acylated and desacylated ghrelin in the plasma of patients with SSc. We also estimated the association between the plasma ghrelin levels and disease phenotypes, such as organ involvement, limited or diffuse cutaneous types and SSc-specific autoantibodies. In addition, we evaluated the biological functions of ghrelin in skin fibroblasts derived from patients with SSc.

2. Patients and methods

2.1. Patients

Blood samples were obtained from 45 Japanese patients with SSc (38 female and 7 male). All patients fulfilled the criteria for SSc proposed by the American College of Rheumatology [22]. Patients were grouped according to the classification system proposed by LeRoy et al. [23]. The baseline characteristics are shown in Table 1. Twenty seven healthy Japanese individuals were enrolled in the present study as HCs (22 female and 5 male; median age: 52 years old). Informed consent was obtained from each patient and each healthy donor.

2.2. Assessment of clinical characteristics

Skin thickness was quantified using the modified Rodnan total skin thickness score (TSS, maximum possible score: 51) [24]. Interstitial lung disease (ILD) was assessed by chest radiography and high-resolution computed tomography (HRCT). Using HRCT, we defined the presence of the following as indicating ILD: a ground-glass appearance, a reticular pattern, and a honeycomb pattern. All patients were assessed by echocardiography, and all patients with a right ventricular systolic pressure of greater than 40 mm Hg underwent right ventricular catheterization. Pulmonary arterial hypertension (PAH) was defined as a mean pulmonary artery pressure of 25 mm Hg or greater and a pulmonary capillary wedge pressure of 15 mm Hg or less at rest [25]. Scleroderma renal crisis (SRC) was defined as malignant arterial hypertension, rapidly progressive renal failure and/or microangiopathic hemolytic anemia (MHA). Patients with hypertension of recent onset without increases in serum creatinine levels or MHA were not categorized as having SRC. A digital ulcer (DU) was defined as a fingertip or toe ulceration that occurred more than once a year. Esophagus involvement was defined as hypomotility shown by barium radiography or esophageal reflux shown by FGS. Intestinal involvement was defined as the presence of malabsorption syndrome, episodes of pseudo-obstruction and/or the need for parenteral hyperalimentation.

Table 1 Baseline characteristics of the patients and healthy controls.

	SSc (n = 45)	HC (n = 27)
Age, years, median (range)	57 (18–73)	52 (32–70)
Gender, female:male	38:7	22:5
Clinical features		
dcSSc, no (%)	36 (80)	
ILD, no (%)	30 (67)	
PAH, no (%)	8 (18)	
SRC, no (%)	3 (7)	
Esophageal reflux, no (%)	37 (82)	
Intestinal involvement, no (%)	2 (4)	
DU, no (%)	16 (36)	
Autoantibodies		
ANA, no (%)	44 (98)	ND
Topo, no (%)	24 (53)	ND
U1RNP, no (%)	8 (18)	ND
CENP, no (%)	9 (20)	ND

SSc, systemic sclerosis; HC, healthy controls; dcSSc, diffuse cutaneous SSc; ILD, interstitial lung disease; PAH, pulmonary arterial hypertension; SRC, scleroderma renal crisis; DU, digital ulcer; ANA, anti-nuclear antibody; Topo, anti-topoisomerase I antibody; CENP, anti-centromere antibody; U1RNP, anti-U1RNP antibody.

2.3. Detection of autoantibodies

The presence of CENP was determined by the distinctive indirect immunofluorescence pattern of HEp-2 cells and by an enzyme immunoassay (MESACUP-2 Test, Medical & Biological Lab, Nagoya, Japan). Both Topo I and U1RNP were determined by double immunodiffusion against calf thymus extracts with commercially available kits (Medical & Biological Lab).

2.4. Measurement of plasma acylated ghrelin and desacylated ghrelin

Blood samples were immediately transferred to chilled polypropylene tubes containing EDTA-2Na (1 mg/ml) and aprotinin (500 U/ml) and centrifuged at 4 °C. Hydrochloride acid (1 N) was added to samples at 10% of the plasma volume immediately after the separation of the plasma, and the plasma sample was stored at −80 °C until assayed. The levels of acylated and desacylated ghrelin were measured using two commercially available enzyme-linked immunosorbent assay (ELISA) kits (Mitsubishi Chemical Medience, Tokyo, Japan). The minimal detection limits of acylated ghrelin and desacylated ghrelin in this assay were 2.5 and 12.5 fmol/ml, respectively.

2.5. Cell culture

Skin biopsies from the dorsal forearm were performed as a diagnostic procedure in 5 patients with SSc. No medical interventions, such as corticosteroids or immunosuppressive agents, were performed before the skin biopsy. The fibroblasts were cultured in Dulbecco's Modified Eagle's medium (DMEM, Invitrogen, Carlsbad, CA) containing 10% fetal bovine serum (Invitrogen). Dermal fibroblasts from passages 3–5 were used for the experiments.

2.6. Measurement of type I collagen

Cultured fibroblasts were prepared at a density of 2×10^4 cells/well in 24-well culture plates with DMEM plus 10% FBS. After 24 h of culture, the medium was removed, and the cells were cultured in serum-free medium (QBSF-51, Sigma-Aldrich, St. Louis, MO). To assess the effect of ghrelin, skin fibroblasts were cultured with recombinant human ghrelin (Peptide Inc., Minoh, Japan) dissolved in phosphate-buffered saline at concentrations of 10–1000 nM for 24–72 h. The supernatants were collected and stored at −80 °C. Procollagen type I C-peptide was measured using an ELISA kit (Takara Shuzo, Kyoto, Japan).

2.7. Quantitative reverse transcription-polymerase chain reaction (RT-PCR)

RNAs were extracted using TRIzol Reagent (Invitrogen) according to the manufacturer's instructions. For the real-time PCR analysis, total RNA was treated with DNase I (Invitrogen), and cDNA was generated using SuperScript III (Invitrogen) with oligo dT primers. The real-time PCR analysis was conducted on Chromo4 (Bio-Rad, Hercules, CA) using the TaqMan Gene Expression Assays (Applied Biosystems, Foster City, CA) for *GHSR1A*, *COL1A2*, *TGFB* and *GAPDH*.

2.8. GHSR1 expression in SSc fibroblasts

GHSR1 expression was analyzed by immunohistochemical staining. Briefly, SSc skin fibroblasts were plated on an 8-chamber slide, cultured for 72 h and used for immunostaining. The samples were washed three times with PBS and fixed in 2% paraformaldehyde (PFA) (Alfa Aesar, Ward Hill, MA) and 0.1% Triton X-100 (Sigma-Aldrich) in PBS for 1 h. After washing three times with PBS, the cells were incubated with a blocking solution (Dako Japan, Tokyo, Japan) for 20 min at room temperature. Excess blocking solution was drained, and the samples were incubated with anti-GHSR1a antibodies (Phoenix Pharmaceuticals Inc., Burlingame, CA) for 30 min at room temperature. The samples were then rinsed with PBS and incubated with a biotinylated secondary antibody (Vector Lab, Burlingame, CA) for 30 min. The staining was developed using the diaminobenzidine substrate (Dako Japan), and counterstaining was performed with hematoxylin. The samples were photographed with a photomicroscope (Olympus, Tokyo, Japan).

2.9. Statistical analysis

A *student's t*-test was used to compare plasma acylated ghrelin and desacylated ghrelin levels, and Fisher's exact probability test was used to compare the frequencies of 2 groups. The Mann–Whitney U test was used to compare the total skin thickness score (TSS) between the 2 groups of patients with SSc. A probability (P) value of <0.05 was considered significant.

3. Results

3.1. Plasma ghrelin levels in SSc

The levels of acylated ghrelin and desacylated ghrelin in the plasma samples from patients with SSc and the HCs were assessed by ELISA (Figs. 1A and B). The levels of plasma acylated ghrelin were 13.6 ± 6.3 fmol/ml in the patients with SSc and 22.7 ± 8.8 fmol/ml in the HCs. The levels of plasma desacylated ghrelin were 72.8 ± 38.6 fmol/ml in the patients with SSc and 152.9 ± 84.5 fmol/ml in the HCs. Both acylated ghrelin and desacylated ghrelin concentrations were significantly lower in the patients with SSc than in the HCs ($P < 0.0001$). The ratio of acylated ghrelin and desacylated ghrelin was not different between the patients with SSc and the HCs (Fig. 1C).

In the SSc subgroups, the levels of acylated ghrelin in the patients with dcSSc ($P < 0.0001$) and lcSSc ($P = 0.035$) were significantly lower than those in the HCs (Fig. 2A). There were no significant differences in the plasma acylated ghrelin levels between the patients with dcSSc and those with lcSSc ($P = 0.27$, Fig. 2A).

3.2. Association between the clinical features of patients with SSc and plasma ghrelin levels

Fibrosis and endothelial injury are the central manifestations of SSc. To investigate which of these manifestations is associated with ghrelin levels, we estimated the association

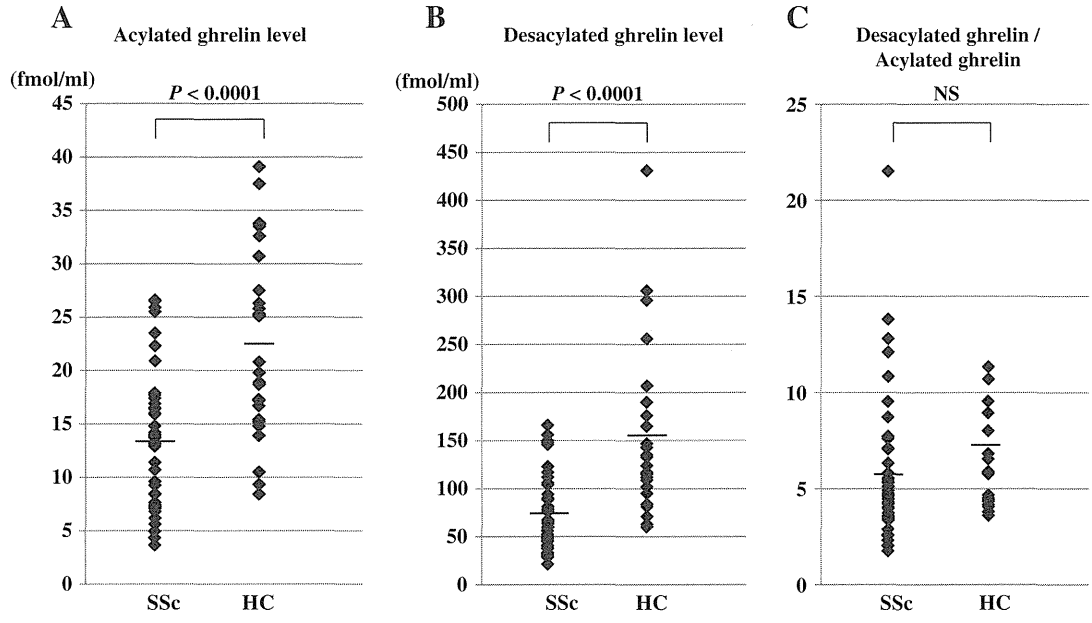

Figure 1 Levels of acylated ghrelin (A) and desacylated ghrelin (B) and the ratio of acylated to desacylated ghrelin (C) in patients with systemic sclerosis (SSc). The levels of both acylated and desacylated ghrelins were significantly decreased in patients with SSc ($P < 0.0001$) compared with healthy controls (HC). The ratio of acylated to desacylated ghrelin in patients with SSc was similar to that in HC.

between the acylated ghrelin level and the clinical manifestations, such as skin fibrosis, ILD, PAH, SRC, esophageal reflux, intestinal involvement, DU, and autoantibodies. Values lower than the mean −1 SD (13.9 fmol/l) of the levels of acylated ghrelin in healthy individuals were considered to be an abnormally low range. We assessed the clinical features between the low and normal levels of acylated ghrelin in patients with SSc. As shown in Table 2, decreased acylated ghrelin levels

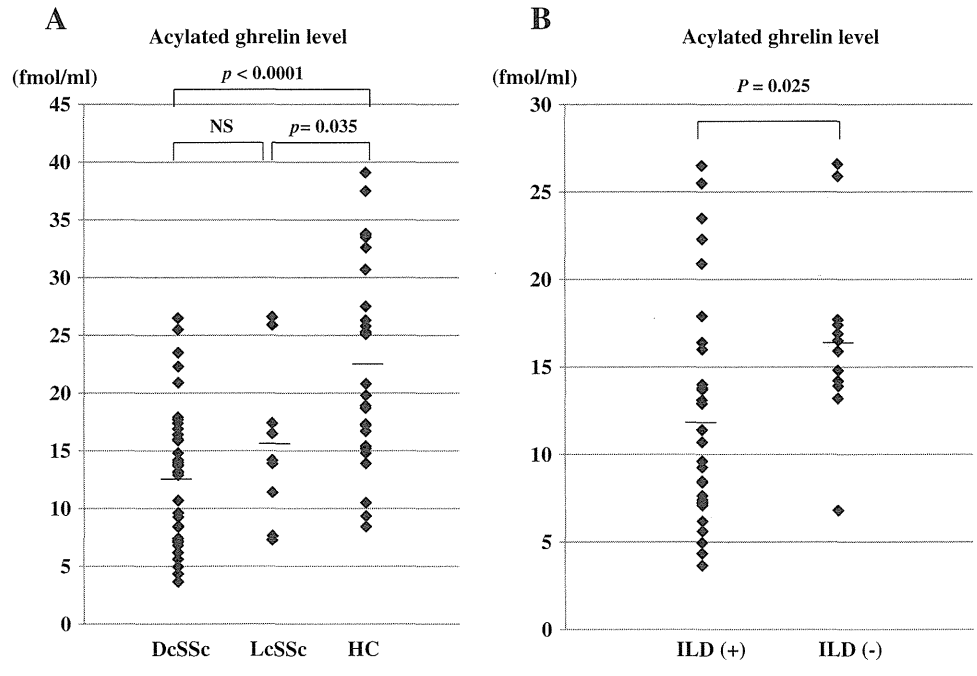

Figure 2 Levels of acylated ghrelin in patients with systemic sclerosis (SSc). (A) The concentrations of acylated ghrelin were measured in both diffuse cutaneous type (dcSSc) and limited cutaneous type (lcSSc). There was no significant difference in the levels of acylated ghrelin between dcSSc and lcSSc. (B) The concentrations of acylated ghrelin were measured in SSc patients with and without interstitial lung disease (ILD). The levels of acylated ghrelin in patients with SSc and ILD were significantly higher than those in patients with SSc in the absence of ILD ($P = 0.025$).

Table 2 Clinical and laboratory findings among SSc patients with elevated acylated ghrelin levels.

	Acylated ghrelin ≤13.9 fmol/ml	Acylated ghrelin >13.9 fmol/ml	*P*	OR	95% CI
Number of patients	24	21			
Sex, M:F	5:19	2:19			
Disease pattern, D:L	20:4	16:5	0.55	1.6	0.4–6.8
Clinical features					
TSS, mean ± SD	22 ± 9	16 ± 9	0.081		
Organ involvement					
ILD, no (%)	21 (88)	9 (43)	0.0015	9.3	2.1–41.3
PAH, no (%)	6 (25)	2 (10)	0.18	3.2	0.6–17.8
SRC, no (%)	2 (8)	1 (5)	0.63	1.8	0.2–21.6
Esophagus, no (%)	20 (83)	17 (81)	0.83	1.2	0.3–5.4
Intestinal involvement, no (%)	2 (8)	0 (0)	0.18	–	–
DU, no (%)	7 (29)	9 (43)	0.45	0.6	0.2–2.2
Autoantibodies					
ANA, no (%)	24 (100)	20 (95)	0.28	–	–
Topo, no (%)	14 (58)	10 (48)	0.47	1.5	0.5–5.0
U1RNP, no (%)	4 (17)	4 (19)	0.83	0.9	0.2–3.9
CENP, no (%)	3 (13)	6 (29)	0.18	0.4	0.1–1.7

TSS, total skin thickness score; ILD, interstitial lung disease; PAH, pulmonary arterial hypertension; SRC, scleroderma renal crisis; DU, digital ulcer; ANA, anti-nuclear antibody; Topo, anti-topoisomerase I antibody; CENP, anti-centromere antibody; U1RNP, anti-U1RNP antibody.

were observed in 53% (24/45) of all SSc patients, 56% (20/36) of dcSSc patients, and 56% (4/9) of lcSSc patients. The frequency of ILD in patients with decreased acylated ghrelin levels was significantly higher than that in patients with normal acylated ghrelin levels (88% versus 43%; $P = 0.0015$, OR: 9.3; 95% CI: 2.1–41.3).

Consistent with these observations, the plasma levels of acylated ghrelin were significantly lower in SSc patients with ILD than those without ILD ($P = 0.025$, Fig. 2B). Additionally, the TSS values in patients with decreased acylated ghrelin levels showed a tendency to be higher than those in patients with normal acylated ghrelin levels ($P = 0.081$, Table 2).

3.3. GHSR1A expression in skin fibroblasts of patients with SSc

To estimate the expression of GHSR1a (the growth hormone secretagogue receptor 1a), which is a ligand of acylated ghrelin in skin fibroblasts, we examined the mRNA and protein levels. As shown in Fig. 3A, the *GHSR1A* was expressed at the transcriptional level in skin fibroblasts from both SSc patients and normal individuals, and there was no difference in the expression levels between the two groups. Immunohistochemical staining using a specific anti-GHSR1a antibody revealed that the expression of GHSR1a was detected in cultured skin fibroblasts from both SSc patients and normal controls (Fig. 3B).

3.4. Effects of ghrelin on collagen production in skin fibroblasts derived from patients with SSc

Thus, we explored the effects of ghrelin on collagen production in skin fibroblasts derived from patients with SSc. Skin fibroblasts derived from 5 patients with SSc were used in the present study. In the experiments in vitro, procollagen type I C-peptide production was significantly suppressed by 100 nM and 1 μM ghrelin in cultured SSc fibroblasts for 72 h ($P < 0.05$, Fig. 4). To determine whether the inhibitory effect of ghrelin on collagen type I occurred at the transcription or post-transcription level, real-time RT-PCR was performed. The levels of *COL1A2* mRNA were significantly decreased by ghrelin stimulation (Fig. 5A). Because intrinsic TGF-β signal transduction contributes to the development of tissue fibrosis in SSc, the effects of ghrelin on *TGFB1* expression were investigated. The analysis of real-time RT-PCR using specific primers for *TGFB1* revealed the inhibitory effects of ghrelin on the mRNA levels of *TGFB1* (Fig. 5B).

4. Discussion

Ghrelin is a gut hormone that is also produced by extra-intestinal tissues and exerts a variety of pleiotropic effects in parenchymal cells [26]. We measured the plasma ghrelin levels (both acylated and desacylated) in patients with SSc. The present study was the first to show that both acylated and desacylated ghrelin levels were significantly decreased in the plasma from patients with SSc compared with those from healthy donors. The ratio of acylated to desacylated ghrelin was not different between patients with SSc and healthy donors. These findings suggest that the production of total ghrelin in SSc patients is diminished but that enzymatic acylation after translation may be normally regulated in SSc patients as well as healthy individuals. We also showed that the patients with low levels of acylated ghrelin had a significantly higher rate of ILD and that the levels of TSS tended to be associated with low acylated ghrelin levels. These results indicated that the levels of acylated ghrelin were inversely correlated with tissue fibrosis.

Ghrelin is predominantly produced by a distinct type of endocrine cell in the gastric oxyntic glands [27]. Involvement

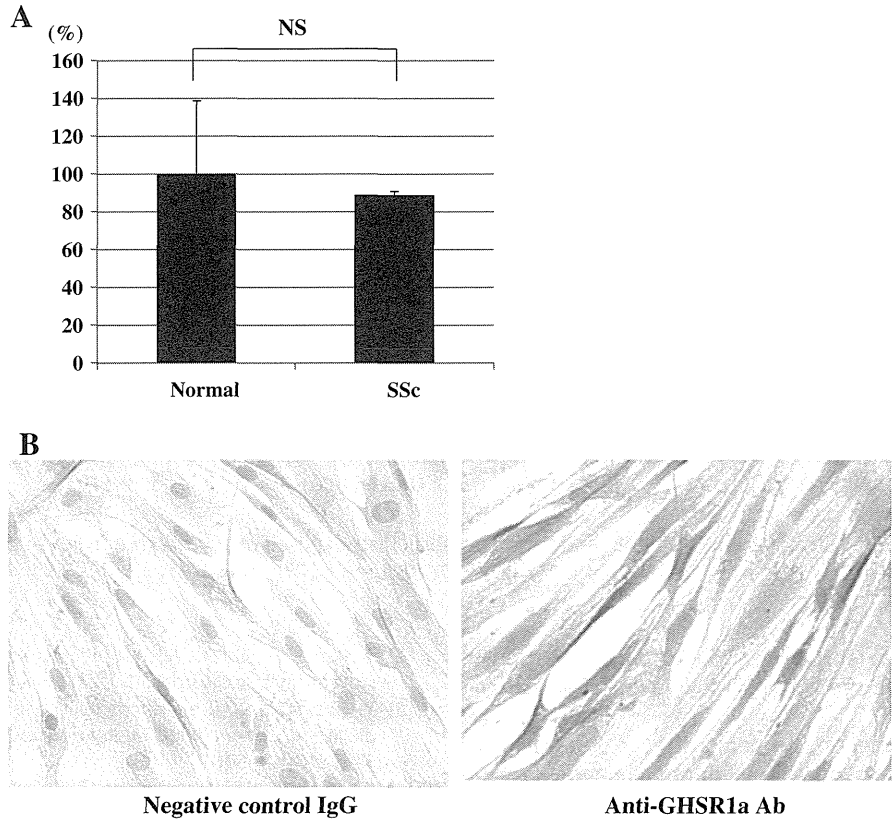

Figure 3 Expression of growth hormone secretagogue receptor (GHSR)1 mRNA and protein in skin fibroblasts. (A) RT-PCR demonstrated the presence of *GHSR1A* mRNA in skin fibroblasts from both systemic sclerosis (SSc) patients and normal individuals, and there was no difference in the expression levels between the two groups. (B) The expression of GHSR1a in skin fibroblasts derived from patients with SSc was estimated by immunohistochemistry. The left panel shows the staining using the negative control IgG, and the right panel shows positive staining using the anti-GHSR1a antibody.

of the upper intestinal tracts, including the esophagus and stomach, is a common complication in patients with SSc [8]. The clinical features of the stomach are gastroparesis and telangiectasia, resulting in atrophy of the acid-secreting mucosa with a resultant loss of feedback to antral gastrin release [28]. These patients frequently had atrophy of the

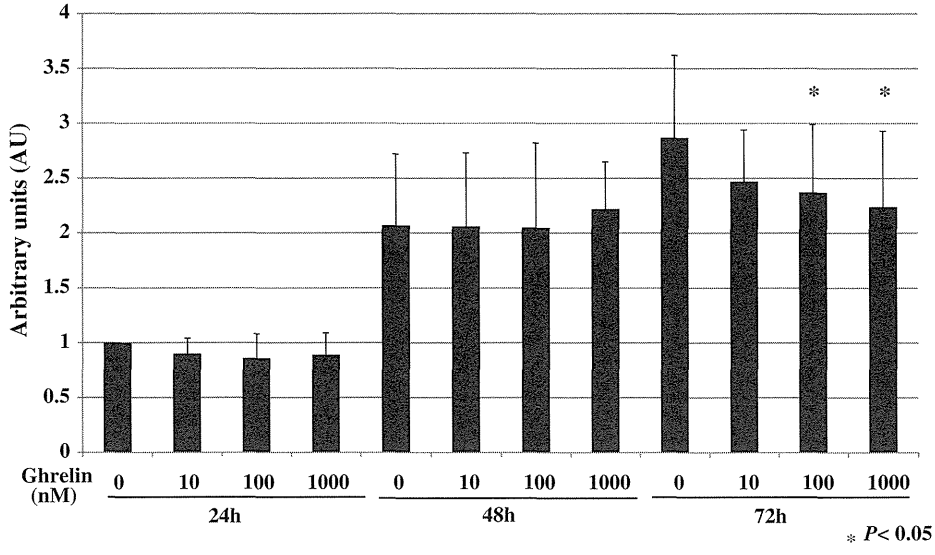

Figure 4 Effect of ghrelin on collagen production in cultured skin fibroblasts from patients with systemic sclerosis (SSc). The fibroblasts were exposed to 0–1000 nM ghrelin for 24–72 h. In 72 h, recombinant ghrelin diminished the production of collagen type I in a dose-dependent manner.

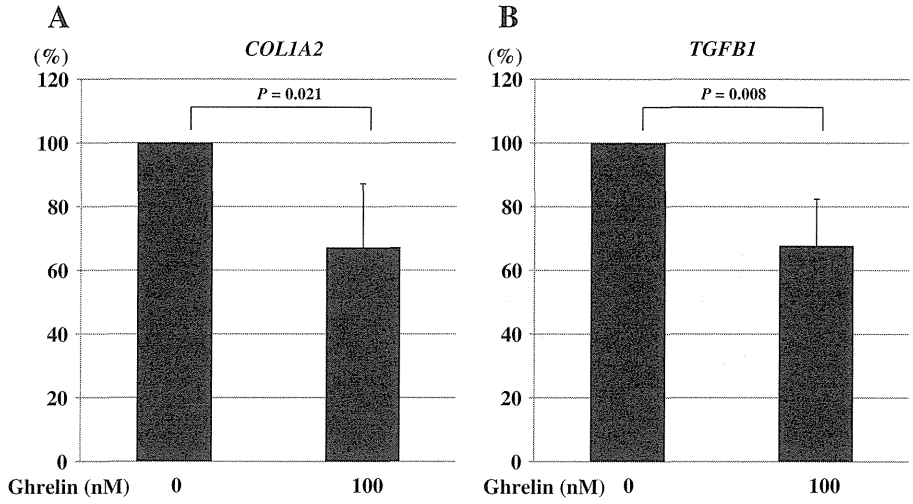

Figure 5 Expression of COL1A2 (A) and *TGFB1* (B) mRNAs in skin fibroblasts exposed to 100 nM ghrelin for 24 h. Recombinant ghrelin exerted the inhibitory effects in the transcription of *COL1A2* and *TGFB1*.

oxyntic gland mucosa. This clinical background in patients with SSc could explain the strikingly low levels of ghrelin in the blood.

In in vitro experiments, we demonstrated for the first time that recombinant ghrelin inhibited collagen type I production in skin fibroblasts. We provided evidence that ghrelin directly reduces collagen synthesis at the mRNA level in cultured skin fibroblasts. However, our observations indicated that ghrelin also exerted inhibitory effects on TGF-β1 expression, which may play a central role in the tissue fibrosis in SSc [29–31]. Taken together, ghrelin may be a potent regulator to suppress fibrosis directly and through the inhibition of TGF-β1.

In 2010, Moreno and colleagues reported that ghrelin reduced the expression of collagen type I and TGF-β1 in hepatic stellate cells, suggesting that ghrelin may be a candidate to treat hepatic fibrosis [32]. More recently, ghrelin was reported to ameliorate bleomycin-induced acute lung injury, which is a mouse model of lung fibrosis [33]. That report indicated that ghrelin suppressed various cytokines and growth factors and prolonged the survival of the bleomycin-treated mice. The authors suggested a novel attractive therapeutic strategy for the treatment of acute lung injury.

In conclusion, the levels of plasma ghrelin might be well inversely correlated to the severity of the fibrosis. Ghrelin exhibited an anti-fibrotic effect in skin fibroblasts in vitro. The administration of ghrelin could be a novel strategy for the treatment of skin and lung fibrosis in patients with SSc.

Conflict of interest statement

The author(s) declare that there are no conflicts of interest.

References

[1] T.A. Medsger Jr., Systemic sclerosis (scleroderma): clinical aspects, in: W.J. Koopman (Ed.), Arthritis and Allied Conditions, 14th ed., Lippincott Williams & Wilkins, Philadelphia, PA, 2001, pp. 1590–1624.

[2] J. Varga, D. Abraham, Systemic sclerosis: a prototype multisystem fibrotic disorder, J. Clin. Invest. 117 (2007) 557–567.

[3] Y. Hamaguchi, Autoantibody profile in systemic sclerosis: predictive value for clinical evaluation and prognosis, J. Dermatol. 37 (2010) 42–53.

[4] A. Gabrielli, E.V. Avvediment, T. Krieg, Sclerodema, N. Engl. J. Med. 360 (2009) 1989–2003.

[5] T.R. Katsumoto, M.L. Whitfield, M.K. Connolly, The pathogenesis of systemic sclerosis, Annu. Rev. Pathol. 6 (2011) 509–537.

[6] A. Usategui, M.J. del Rey, J.L. Pablos, Fibroblast abnormalities in the pathogenesis of systemic sclerosis, Expert. Rev. Clin. Immunol. 7 (2011) 491–498.

[7] R. Domsic, K. Fasanella, K. Bielefeldt, Gastrointestinal manifestations of systemic sclerosis, Dig. Dis. Sci. 53 (2008) 1163–1174.

[8] A. Forbes, I. Marie, Gastrointestinal complications: the most frequent internal complications of systemic sclerosis, Rheumatology 48 (Suppl. 3) (2009) iii36–iii39.

[9] C.P. Denton, C.M. Black, D.J. Abraham, Mechanisms and consequences of fibrosis in systemic sclerosis, Nat. Clin. Pract. Rheumatol. 2 (2006) 134–144.

[10] M. Kojima, H. Hosoda, Y. Date, M. Nakazato, H. Matuo, K. Kangawa, Ghrelin is a growth-hormone-releasing acylated peptide from stomach, Nature 402 (1999) 656–660.

[11] H. Hosoda, M. Kojima, H. Matsuo, K. Kangawa, Ghrelin and des-acylated ghrelin: two major forms of rat ghrelin peptide in gastrointestinal tissue, Biochem. Biophys. Res. Commun. 279 (2000) 1077–1080.

[12] C. De Vriese, F. Gregoire, R. Lema-Kisoka, M. Waelbroeck, P. Robberecht, C. Delporte, Ghrelin degradation by serum and tissue homogenates: identification of the cleavage sites, Endocriology 145 (2004) 4997–5005.

[13] S. Gnanapavan, B. Kola, S.A. Bustin, D.G. Morris, P. McGee, P. Fairclough, et al., The tissue distribution of the mRNA of ghrelin and subtypes of its receptor, GHS-R, in humans, J. Clin. Endocrinol. Metab. 87 (2002) 2988–2991.

[14] A.M. Wren, S.R. Bloom, Gut hormones and appetite control, Gastroenterology 132 (2007) 2116–2130.

[15] W.G. Li, D. Gavrila, X. Liu, L. Wang, S. Gunnlaugsson, L.L. Stoll, et al., Ghrelin inhibits proinflammatory responses and nuclear factor kappaB activation in human endothelial cells, Circulation 109 (2004) 2221–2226.

[16] V.D. Dixit, E.M. Schaffer, R.S. Pyle, G.D. Collins, S.K. Sakthivel, R. Palaniappan, et al., Ghrelin inhibits leptin- and activation-induced proinflammatory cytokine expression by

human monocytes and T cells, J. Clin. Invest. 114 (2004) 57–66.
[17] T. Shinya, M. Nakazato, M. Mizuta, Y. Date, M.S. Mondal, M. Tanaka, et al., Plasma ghrelin levels in lean and obese humans and the effect of glucose on ghrelin secretion, J. Clin. Endocrinol. Metab. 87 (2002) 240–244.
[18] N. Nagaya, M. Uematsu, M. Kojima, Y. Date, M. Nakazato, H. Okamura, et al., Elevated circulating levels of ghrelin in cachexia associated with chronic heart failure: relationships between ghrelin and anabolic/catabolic factors, Circulation 104 (2001) 2034–2038.
[19] Suleyman Serdar Koca, Metin Ozgen, Suleyman Aydin, Sait Dag, Bahri Evren, Ahmet Isik, Ghrelin and obestatin levels in rheumatoid arthritis, Inflammation 31 (2008) 329–335.
[20] P. Kumper, R. Horn, G. Brabant, A. Woywodt, M. Schiffer, H. Haller, M. Haubitz, Serum leptin and ghrelin correlate with disease activity in ANCA-associated vasculitis, Rheumatology 47 (2008) 484–487.
[21] H. Takeda, C. Sadakane, T. Hattori, T. Katsurada, T. Ohkawara, K. Nagai, et al., Rikkunshito, an herbal medicine, suppresses cisplatin-induced anorexia in rats via 5-HT2 receptor antagonism, Gastroenterology 134 (2008) 2004–2013.
[22] Subcommittee for Scleroderma Criteria of the American Rheumatism Association Diagnostic and Therapeutic Criteria Committee. Preliminary criteria for the classification of systemic sclerosis (scleroderma), Arthritis Rheum. 23 (1980) 581–590.
[23] E.C. LeRoy, C. Black, R. Fleischmajer, S. Jablonska, T. Krieg, T.A. Medsger Jr., et al., Scleroderma (systemic sclerosis): classification, subsets and pathogenesis, J. Rheumatol. 15 (1988) 202–205.
[24] P. Clements, P. Lachenbruch, J. Siebold, B. White, S. Weiner, R. Martin, et al., Inter and intraobserver variability of total skin thickness score (modified Rodnan TSS) in systemic sclerosis, J. Rheumatol. 22 (1995) 1281–1285.
[25] N. Galie, M.M. Hoeper, M. Humbert, A. Torbicki, J.L. Vachiery, J.A. Barbera, et al., Guidelines for the diagnosis and treatment of pulmonary hypertension: The task force for the diagnosis and treatment of pulmonary hypertension of the European Society of Cardiology (ESC) and the European Respiratory Society (ERS), endorsed by the International Society of Heart and Lung Transplantation (ISHLT), Eur. Heart J. 30 (2009) 2493–2537.
[26] A.J. Van der Lely, M. Tschop, M.I. Heiman, E. Ghigo, Biological, physiological, pathophysiological, and pharmacological aspects of ghrelin, Endocr. Rev. 25 (2004) 426–457.
[27] Y. Date, M. Kojima, H. Hosoda, A. Sawagashira, M.S. Mondal, T. Suganuma, et al., Ghrelin, a novel growth hormone-releasing acylated peptide, is synthesized in a distinct endocrine cell type in the gastrointestinal tracts of rats and humans, Endocrinology 141 (2000) 4255–4261.
[28] E.C. Ebert, Gastric and enteric involvement in progressive systemic sclerosis, J. Clin. Gastroenterol. 42 (2008) 5–12.
[29] A. Jelaska, J.H. Korn, Role of apoptosis and transforming growth factor beta1 in fibroblasts selection and activation in systemic sclerosis, Arthritis Rheum. 43 (2000) 2230–2239.
[30] M. Jinnin, Mechanisms of skin fibrosis in systemic sclerosis, J. Dermatol. 37 (2010) 11–25.
[31] J. Varga, B. Pasche, Transforming growth factor beta as a therapeutic target in systemic sclerosis, Nat. Rev. Rheumatol. 5 (2009) 200–206.
[32] M. Moreno, J.F. Chaves, P. Sancho-Bru, F. Ramalho, L.N. Ramalho, M.L. Mansego, et al., Ghrelin attenuates hepatocellular injury and liver fibrogenesis in rodents and influences fibrosis progression in humans, Hepatology 51 (2010) 974–985.
[33] Y. Imazu, S. Yanagi, K. Miyoshi, H. Tsubouchi, S. Yamashita, N. Matsumoto, et al., Ghrelin ameliorates bleomycin-induced acute lung injury by protecting alveolar epithelial cells and suppressing lung inflammation, Eur. J. Pharmacol. 672 (2011) 153–158.

Masuda et al. Arthritis Research & Therapy 2013, 15:R74
http://arthritis-research.com/content/15/4/R74

arthritis research&therapy

RESEARCH ARTICLE Open Access

Versican is upregulated in circulating monocytes in patients with systemic sclerosis and amplifies a CCL2-mediated pathogenic loop

Ayako Masuda[1], Hidekata Yasuoka[1], Takashi Satoh[1], Yuka Okazaki[1], Yukie Yamaguchi[1,2] and Masataka Kuwana[1*]

Abstract

Introduction: Altered phenotypes of circulating monocytes of patients with systemic sclerosis (SSc) have been reported, but the role of these alterations in the pathogenesis of SSc remains unclear. This study was undertaken to identify molecules that are preferentially expressed by SSc monocytes, and to investigate the roles of these molecules in the pathogenic process of SSc.

Methods: We analyzed circulating $CD14^+$ monocytes isolated from 36 patients with SSc and 32 healthy control subjects. The monocytes' gene expression profiles were assessed by Oligo GEArray® (SABiosciences, Frederic, MA, USA) and semiquantitative or quantitative PCR; their protein expression was evaluated in culture supernatants of unstimulated monocytes by immunoblotting or ELISA, and by immunocytostaining. Monocyte chemoattractant activity of CCL2 was assessed in a TransWell® system (Corning Incorporated, Corning, NY, USA) in the presence or absence of chondroitin sulfate (CS).

Results: A step-wise approach to profiling gene expression identified that versican and CCL2 were upregulated in SSc monocytes. Subsequent analysis of proteins expressed in monocyte culture supernatants confirmed enhanced production of versican and CCL2 in SSc monocytes compared with control monocytes. CCL2 bound to CS chains of versican and colocalized with versican in the monocytes' Golgi apparatus. Finally, CCL2 had a greater ability to mediate monocyte migration when bound to CS chains, because this binding provided efficient formation of CCL2 gradients and protection from protease attack.

Conclusion: Circulating monocytes with elevated versican and CCL2 levels may contribute to the fibrotic process in a subset of SSc patients by amplifying a positive feedback loop consisting of versican, CCL2, and the influx of monocytes.

Keywords: systemic sclerosis, monocytes, versican, CCL2

Introduction

Systemic sclerosis (SSc) is a multisystem disease characterized by microvascular abnormalities and excessive fibrosis [1]. Current research suggests that the pathogenic process of SSc damages endothelial cells and activates immune cells and fibroblasts, causing excessive accumulation of extracellular matrix (ECM) [2]. Mononuclear cell infiltration, consisting predominantly of macrophages and T cells, has been detected histopathologically in SSc lesions in the skin, lung, and other tissues, especially in the early phases of SSc [3,4]. Tissue macrophages in the perivascular skin express activation markers such as HLA-DR, platelet-derived growth factor B receptor [5], and CD163 [6]. Activated macrophages in the skin express CD204 [6], a marker for the M2 macrophages that are associated with wound repair and fibrotic conditions [7]. A recent study of lung tissue in SSc patients with interstitial lung disease found prominent infiltrates of fibrocytes expressing CD34, CD45, and collagen type I [8]; precursors of cells expressing these markers are found among circulating $CD14^+$ monocytes [9]. These findings indicate

* Correspondence: kuwanam@z5.keio.jp
[1]Department of Internal Medicine, Keio University School of Medicine, 35 Shinanomachi, Shunjuku, Tokyo 160-8582, Japan
Full list of author information is available at the end of the article

that monocytes and monocyte-lineage cells are actively involved in the pathophysiology of SSc.

Circulating $CD14^+$ monocytes derive from hematopoietic stem cells in the bone marrow and migrate to their ultimate sites of activity, and form a heterogeneous population in terms of surface markers, phagocytic capacity, and differentiation potential. Although circulating monocytes are committed precursors with the capacity to differentiate into a variety of phagocytes, including macrophages and dendritic cells, there is growing evidence that these monocytes can differentiate into other cell types as well, including cells with the typical characteristics of endothelial cells and fibroblasts [10-13]. Circulating monocytes are now recognized as multifunctional precursors, playing critical roles not only in immune and inflammatory responses but also in tissue regeneration and in pathologic tissue remodeling, such as excessive fibrosis and tumor development [13,14].

$CD14^+$ monocytes are increased in peripheral blood of SSc patients [6], and the molecular phenotypes and the proportions of cell types in the population are altered, with a larger proportion of type I collagen-producing monocytes [15], $CXCR4^+$ circulating cells with monocytic and endothelial features [16], monocytic proangiogenic hematopoietic cells [17], and $CD163^+CD204^+$ cells with a profibrotic M2 phenotype [6]. Moreover, recent microarray analyses of circulating monocytes identified several genes that are overexpressed in SSc monocytes, including type I interferon-regulated genes such as Siglec-1 [18,19]. The SSc pathogenic process thus probably recruits circulating monocytes to the affected sites, where they acquire profibrotic properties. Although the details are still unclear, there may be at least two distinct mechanisms underlying profibrotic properties of these monocytes - the production of a variety of profibrotic growth factors, cytokines, and chemokines, including transforming growth factor beta and platelet-derived growth factor [2], and their transdifferentiation into ECM-producing cells [10,11,20].

In this study, we evaluated the gene and protein expression profiles of circulating $CD14^+$ monocytes in patients with SSc, using a high-throughput platform. We were particularly interested in genes related to ECM metabolism, chemokines, and their receptors, or endothelial cell function.

Materials and methods

Patients and controls

This study included 36 patients (four men and 32 women) who met the preliminary SSc classification criteria proposed by the American College of Rheumatology [21]. Using the published criteria, 19 patients were classified as having diffuse cutaneous SSc (dcSSc) and 17 as having limited cutaneous SSc (lcSSc) [22]. The study included 32 healthy control subjects (16 men and 16 women). The average age at the time of examination was 55.3 ± 15.9 in SSc patients and 45.8 ± 19.3 in control subjects.

Organ involvement related to SSc was defined for each patient as described previously [23]. SSc-related autoantibodies were identified by indirect immunofluorescence using commercially prepared slides of monolayer HEp-2 cells (MBL, Nagano, Japan) and immunoprecipitation assays [23]. The mean disease duration from onset of Raynaud's phenomenon was 13.6 ± 10.4 years. In patients with dcSSc, 13 of 19 were in late phase, with disease duration >5 years from the onset of non-Raynaud's phenomenon symptoms. Table 1 presents patients' autoantibody profiles, SSc-related organ involvement, and medications reported at the time of blood collection. Before collecting blood samples, we obtained written, informed consent from both patients and control subjects in accord with the tenets of the Declaration of Helsinki, and as approved by the International Review Board of Keio University.

Table 1 Clinical characteristics of 36 patients with systemic sclerosis

Characteristic	*n* (%)
Organ involvement	
Joint contractures	16 (44%)
Esophageal hypomotility	24 (67%)
Cardiac involvement	1 (3%)
Renal involvement	1 (3%)
Interstitial lung disease	22 (62%)
Pulmonary arterial hypertension	1 (3%)
Digital pitting scars	18 (50%)
Systemic sclerosis-related autoantibodies[a]	
Anti-topoisomerase I	16 (44%)
Anticentromere	7 (19%)
Anti-RNA polymerase III	2 (6%)
Anti-U1 ribonucleoprotein	7 (19%)
Anti-Th/To	2 (6%)
Not identified	5 (14%)
Medications reported when blood samples collected	
Prednisolone (≤10 mg/day)	11 (31%)
Cyclophosphamide	1 (3%)
Nonsteroidal anti-inflammatory drug	5 (14%)
D-Penicillamine	3 (8%)
Oral prostanoid	19 (53%)
Calcium channel blocker	2 (6%)
Statin	6 (17%)
Anti-platelet aggregation	6 (17%)
Antacid	12 (33%)

[a]Three patients had two systemic sclerosis-related autoantibodies: one patient with anti-topoisomerase I and anticentromere; one patient with anti-topoisomerase I and anti-U1 ribonucleoprotein; and one patient with anticentromere and anti-U1 ribonucleoprotein.

Cell preparation

Peripheral blood mononuclear cells (PBMCs) were isolated from heparinized venous blood by Lymphoprep™ (Fresenius Kabi Norge, Halden, Norway) density-gradient centrifugation. $CD14^+$ monocytes were separated from PBMCs using an anti-CD14 mAb coupled to magnetic beads (CD14 MicroBeads; Miltenyi Biotech, Bergisch Gladbach, Germany) followed by magnetic cell sorting column separation according to the manufacturer's protocol [24]. Flow cytometric analysis showed that the sorted fraction consistently contained more than 95% $CD14^+$ cells.

Gene expression profiling

Total RNA was extracted from purified monocytes using the ArrayGrade™ Total RNA Isolation kit (SABiosciences, Frederic, MA, USA) according to the manufacturer's protocol. Pooled RNA was prepared by mixing equal amounts of total RNA from five patients with SSc or from five healthy control subjects. We prepared two different independent sets of RNA. The first SSc patient set was composed of RNA from four females and one male with dcSSc (mean age at examination 40.0 ± 12.3, and mean disease duration from onset of Raynaud's phenomenon 9.4 ± 7.1 years). The second set was derived from four females and one male (four dcSSc and one lcSSc, mean age at examination 50.4 ± 8.9, and mean disease duration 16.2 ± 10.6 years). We generated biotin-16-uridine-5'-triphosphate-labeled cRNA probes from pooled total RNA (3 μg) using reverse transcription and a TrueLabeling-AMP™ 2.0 kit (SABiosciences). Gene expression was profiled from pooled total RNA (3 μg) using Oligo GEArray® (SABiosciences) according to the manufacturer's instructions. This array covers 330 genes encoding ECM and adhesion molecules, chemokines and receptors, and proteins with endothelial cell functions.

The intensity of individual bands was measured by densitometry with National Institute of Health image software (Image J; National Institute of Mental Health, Bethesda, MD, USA). Relative gene expression levels were calculated as a ratio of the intensity of the target spot to that of glyceraldehyde-3-phosphate dehydrogenase. To identify genes that were upregulated in SSc monocytes, we compared the expression levels of individual genes in two independent sets of pooled monocyte RNA obtained from five SSc patients and from five healthy subjects. We selected candidate genes that met both of the following criteria: they were expressed at higher levels in SSc than in control monocytes in two independent sets, and they had 1.5-fold greater expression in SSc than in healthy monocytes in at least one set [25].

Semiquantitative and quantitative PCR

Total RNA was extracted from monocytes using an RNeasy® mini kit (Qiagen Inc, Valencia, CA, USA), first-strand cDNA was reverse-transcribed with an oligo $(dT)_{12\text{-}15}$ primer (Invitrogen, Carlsbad, CA, USA), and cDNA equivalent to 2 ng total RNA was used for PCR analysis. The primer sequences, annealing temperatures, and cycles used to amplify individual genes are summarized in Table 2. Individual band intensity was quantified by densitometry. Relative mRNA expression levels were calculated as a ratio of the band intensity of the target gene to that of glyceraldehyde-3-phosphate dehydrogenase.

Gene mRNA expression levels were further evaluated by quantitative PCR using the TaqMan® real-time PCR system (Applied Biosystems, Foster City, CA, USA) according to the manufacturer's protocols. Each gene's expression was measured relative to glyceraldehyde-3-phosphate dehydrogenase. Specific primers and probes for amplifying genes encoding L-selectin (Hs00174151), versican (Hs00171642), CCL2 (Hs00234140), CXCL8 (Hs00174103), versican V0 isoform (Hs01007944), and versican V1 isoform (Hs01007937) were purchased from Applied Biosystems. In some experiments, high and low mRNA expression levels were defined according to the mean plus two standard deviations of the levels in healthy control samples.

Quantifying proteins in monocyte culture supernatants

Monocytes were plated and cultured in RPMI 1640 containing 10% fetal bovine serum, 50 U/ml penicillin, and 50 μg/ml streptomycin. To measure versican production, 5×10^6 monocytes were cultured in six-well plates without exogenous stimulation. Supernatants were harvested at 48 hours, concentrated with an Ultra-free MC 30K filter (Millipore, Billerica, MA, USA), and treated with chondroitinase ABC (Seikagaku Kogyo, Tokyo, Japan) to cleave chondroitin sulfate (CS) chains. The samples were then analyzed by SDS-PAGE, followed by immunoblotting with mouse mAb to human versican (clone 2B1; Seikagaku Kogyo) and horseradish peroxidase-conjugated goat anti-rabbit secondary antibodies (Thermo Fisher Scientific, Rockford, IL, USA). Bound antibodies were detected with a chemiluminescence detection system (Perkin Elmer Life Sciences, Boston, MA, USA). The signal intensity of the band corresponding to the molecular weight of a truncated versican (250 kDa) was quantified by densitometry. To measure CCL2 production, 10^5 cells were cultured in 24-well plates without exogenous stimulation, culture supernatants were harvested at 24 hours, and CCL2 was measured in culture supernatants using a Quantikine® ELISA kit (R&D Systems, Abingdon, UK).

Immunocytostaining

The intracellular localization of versican and CCL2 was determined by immunofluorescence as reported previously [26]. Briefly, $CD14^+$ monocytes were cultured on BD BioCoat™ Poly-D-Lysine Cellware (BD Biosciences,

Table 2 Primer sequences, annealing temperatures, and cycles used for semiquantitative PCR

Gene	Sense primer (5′ → 3′)	Antisense primer (5′ → 3′)	Annealing temperature (°C)	Cycle
CCL2	agcaagtgtcccaaagaagc	gcaatttccccaagtcctg	66	32
Type I collagen α1	cctggatgccatcaaagtct	ccttcttgaggttgccagtc	66	33
Versican	tcattcaacgtcaccttcca	ggtccaaaaatccaaaccaa	66	34
L-selectin	tcagctgctctgaaggaaca	taaccatgactgccactgga	60	30
CCR1	tcctcacgaaagcctacgaggagagtccaagc	ccacggagaggagggagccatttaac	66	30
CXCL8	cagttttgccaaggagtgct	attgcatctggcaaccctac	63	27
MMP-2	ccaaggagagctgcaacct	ccaaggtccatagctcatcgtc	63	40
CCRL2	ctgggctcatgctggggg	tgcagcagtgggtggtgg	60	30
GAPDH	tgaacgggaagctcactgg	tccaccaccctgttgctgta	60	25
Versican variants				
Versican V0	tcaacatctcatgttctccc	ttcttcactgtgggtataggtcta	57	34
Versican V1	ggctttgaccagtgcgattac	ttcttcactgtgggtataggtcta	57	28
Versican V2	tcaacatctcatgttctccc	ccagccatagtcacatgtctc	65	38
Versican V3	ggctttgaccagtgcgattac	ccagccatagtcacatgtctc	61	32

San Diego, CA, USA) for 2 hours. The cells were fixed with acetone and incubated with goat anti-human versican polyclonal antibodies (Santa Cruz Biotechnology, Santa Cruz, CA, USA) in combination with rabbit anti-human CCL2 polyclonal antibodies (Santa Cruz Biotechnology) or a mouse anti-human goldin-97 mAb (clone CDF4; Invitrogen), followed by incubation with the appropriate secondary antibodies conjugated to Alexa Fluor-488 or Alexa Fluor-568 (Invitrogen). For negative controls, cells were incubated with an isotype-matched mouse or rat mAb against an irrelevant antigen instead of the primary antibody. TO-PRO3 (Invitrogen) was used to counterstain nuclei. Images were taken with a Fluoview FV1000 confocal laser fluorescence microscope (Olympus, Tokyo, Japan).

Assessing capacity of CCL2 for binding chondroitin sulfate

Carbonate buffer (15 mM Na_2CO_3, 10 mM $NaHCO_3$) alone or a solution of synthetic CS (Seikagaku Kogyo) dissolved in carbonate buffer (200 μg/ml) was incubated in 24-well plastic plates overnight at 4°C. Unbound CS was removed, and recombinant CCL2 (50 ng/ml; R&D Systems) was added to the wells and incubated for 2 hours at 37°C. Protein components attached to the plate were recovered with 2% SDS, applied to immunoblots with rabbit anti-CCL2 polyclonal antibody (Abcam, Cambridge, MA, USA), and visualized with a chemiluminescence detection system.

To assess how binding to CS affected CCL2's vulnerability to protease-mediated degradation, we incubated recombinant CCL2 in 24-well plastic plates in the presence or absence of CS at 37°C for 2 hours, and then left the wells untreated or treated them with elastase (2 mM), cathepsin G (1 ml; Calbiochem, San Diego, CA, USA), or trypsin (0.0005%; BD Biosciences) at 37°C for 1 hour. Protein components were recovered and analyzed by immunoblots probed with anti-CCL2 polyclonal antibody. The signal intensity of the band corresponding to intact CCL2 (10 kDa) was semi-quantified using densitometry. The percentage of intact CCL2 in individual samples was expressed as a percentage of that found on pretreated CS-coated wells that did not receive protease treatment.

Migration assay

Monocyte migration was evaluated as described previously [27], with some modifications. Briefly, the lower chambers of 24-well TransWell® plates with 5 μm pore filters (Corning Incorporated, Corning, NY, USA) were left untreated (vehicle) or coated with serial concentrations of CS (10, 50, and 250 μg/ml). The wells were incubated with recombinant CCL2 (50 ng/ml) for 2 hours at 37°C, after which monocytes (3×10^5) were placed in the upper chambers for 2 hours at 37°C with 5% carbon dioxide. Cells in the lower chambers were counted manually using a hemocytometer, and migration ratios were calculated as a percentage of the cells induced to migrate by vehicle alone. All experiments were carried out in duplicate. In some experiments, mouse anti-CCL2 mAb (R&D Systems) or mouse IgG (3.0 ng/ml; Dako, Glostrup, Demark) was added to the lower chamber. The relative monocyte migration in individual experiments was calculated as a percentage of the migration induced in vehicle-coated wells without CCL2.

Statistical analysis

All continuous variables were recorded as mean ± standard deviation, and statistical differences were compared using a nonparametric Mann-Whitney U test. Categorical variables were compared with Fisher's exact test or a chi-square test when appropriate. The correlation

coefficient (r) was determined using a single regression model.

Results

Identifying genes with altered expression in SSc monocytes

We used the Oligo GEarray™ system, which can screen 330 genes associated with ECM and adhesion molecules, chemokines and receptors, and endothelial cell biology, to compare gene expression profiles in circulating monocytes from SSc patients or healthy controls. We performed two independent analysis sets on mixed total RNA samples: one set from five SSc patients and the other from five healthy controls. Based on results of two independent sets of analysis, we selected collagen type I α1, versican, L-selectin, matrix metalloproteinase-2, CCL2, CXCL8, CCR1, and CCRL2 as candidates for genes preferentially overexpressed in SSc monocytes (Figure 1). Of these, only versican was confirmed by semi-quantitative PCR and quantitative TaqMan® real-time PCR to be significantly upregulated in SSc monocytes.

Figure 2 shows versican mRNA levels, quantified by TaqMan® real-time PCR, in monocytes from 24 SSc patients and 13 control subjects (219.9 ± 376.5 vs. 46.2 ± 31.1, $P = 0.002$). Although CCL2 expression tended to be higher in SSc patients, the difference was not statistically significant ($P = 0.06$). Since CCL2 levels in SSc monocytes varied widely, we increased the number of subjects sampled (36 patients with SSc, 32 control subjects) and the difference in CCL2 gene expression between the two groups reached statistical significance (0.37 ± 0.53 vs. 0.11 ± 0.07, $P = 0.04$) (Figure 2). The remaining six candidate genes were excluded because confirmatory analyses did not show a statistically significant difference between their expression levels in SSc and control monocytes.

Clinical features associated with high versican or CCL2 mRNA expression in monocytes

Versican and CCL2 mRNA levels varied considerably among SSc monocytes, and high expression levels were detected in a subgroup of patients. We examined clinical

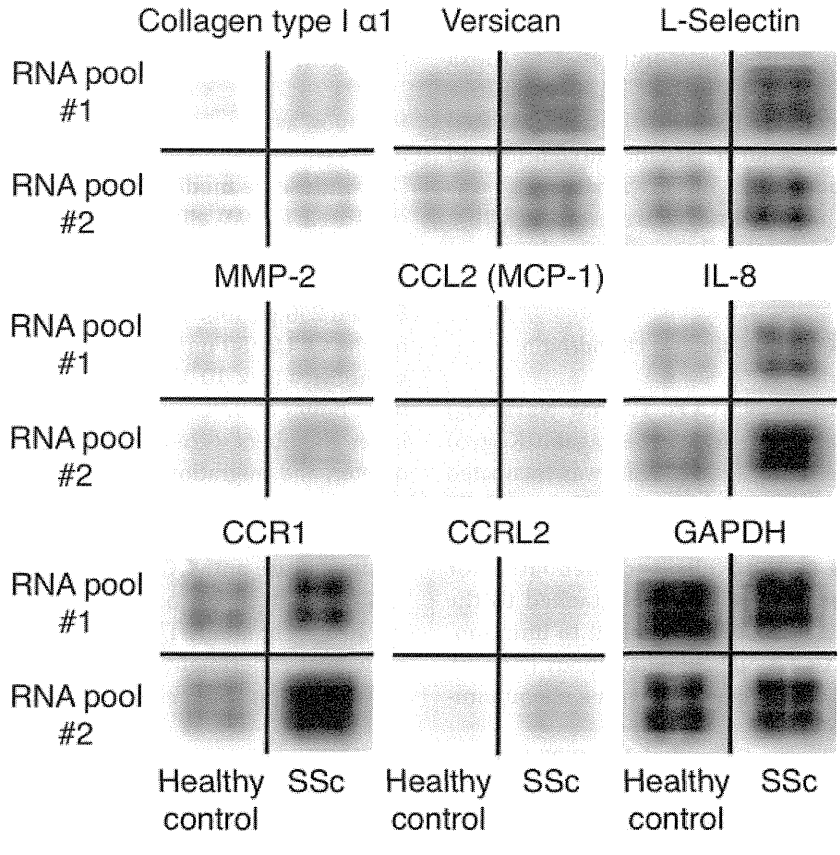

Figure 1 Gene expression profiles of circulating monocytes from patients with systemic sclerosis and from healthy controls. Two sets of genes, each set containing RNA from five subjects, were analyzed (RNA pool #1 and #2) with the Oligo GEArray® (SABiosciences, Frederic, MA, USA). The results for eight candidate genes for genes preferentially overexpressed in systemic sclerosis (SSc) monocytes are shown along with control (glycelaldehyde-3-phosphate dehydrogenase (GAPDH)).

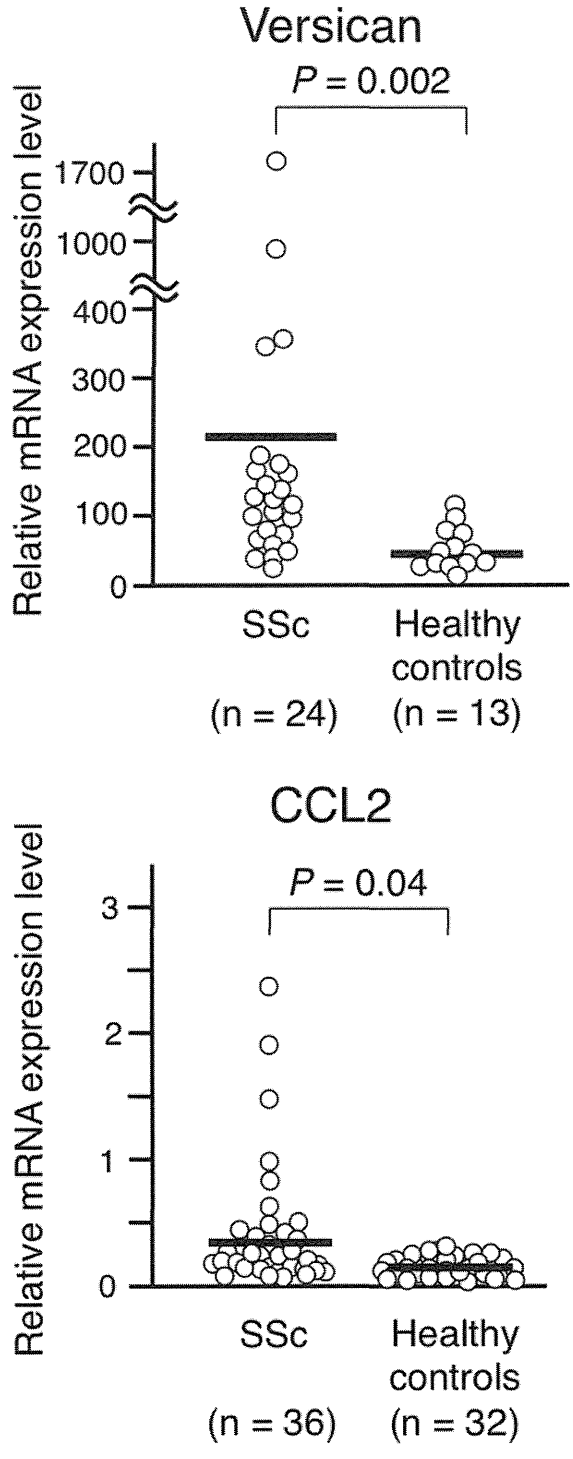

Figure 2 Versican and CCL2 mRNA levels in monocytes from patients with systemic sclerosis and healthy controls. Quantitative PCR analysis. Relative mRNA expression levels were calculated as a ratio of mRNA levels of the genes of interest to those of glyceraldehyde-3-phosphate dehydrogenase (GAPDH). Bars in the graph denote the mean. Differences between the groups were analyzed by Mann-Whitney *U* test. SSc, systemic sclerosis.

features associated with a high level of versican or CCL2 mRNA in circulating monocytes, which were defined based on above the mean plus two standard deviations of the levels in healthy control samples. We examined 24 patients with SSc, 11 with high levels and 13 with low levels of versican expression, and found differences in the frequencies of dcSSc (82% vs. 25%, $P = 0.02$), interstitial lung disease (82% vs. 46%, $P = 0.04$), positive anti-topoisomerase I antibody (64% vs. 15%, $P = 0.01$), and esophageal involvement (100% vs. 46%, $P = 0.006$). In fact, versican levels were significantly higher in patients with dcSSc than in those with lcSSc (413 ± 531 vs. 100 ± 92, $P = 0.03$), and in patients with esophageal involvement than those without (340 ± 459 vs. 54 ± 34, $P = 0.002$). In particular, all four patients with an extremely high mRNA expression level of versican (>300) had dcSSc. We did not find any correlation with clinical characteristics and the level of CCL2 mRNA expressed by circulating monocytes in SSc patients.

Upregulated mRNA expression of the versican isoforms V0 and V1 in SSc monocytes

Versican, or CS proteoglycan 2, is a large extracellular matrix proteoglycan (>1,000 kDa) that is present in a variety of human tissues, including skin and blood vessels [28]. Versican consists of an amino-terminal hyaluronan binding region, a glycosaminoglycan (GAG)-binding domain, and a C-type lectin-like domain. Numerous CS chains are attached to a GAG-binding domain (Figure 3A). In addition to full-length versican (V0), three short isoforms having GAG-binding domains of different sizes (V1, V2, and V3) are generated by alternative splicing (Figure 3B).

We designed PCR primers to detect each of the four versican isoforms separately, and assessed their mRNA levels in SSc and control monocytes. Semiquantitative PCR analysis of monocytes from 30 patients with SSc and 17 healthy controls showed significantly higher mRNA levels of both V0 and V1 in SSc than in control monocytes ($P = 0.01$ for both comparisons), while V2 and V3 levels were comparable in the two groups (Figure 3C).

TaqMan® real-time PCR confirmed that mRNA expression of the V0 and V1 isoforms, both of which have long GAG-binding domains, was upregulated in SSc patients as compared with healthy control subjects (Figure 4).

Versican and CCL2 proteins are upregulated in SSc monocytes

We cultured freshly isolated monocytes without any exogenous stimuli, and measured versican and CCL2 proteins spontaneously secreted into the supernatant during cultures. As shown in Figure 5A, the versican V0 isoform was concentrated and detected in supernatants by immunoblotting. Versican levels were significantly higher in culture supernatants from SSc monocytes than in those from healthy control monocytes ($P = 0.03$) (Figure 5B). SSc monocytes also produced more CCL2 than did control monocytes ($P = 0.01$) (Figure 5C). The mRNA and protein expression levels in a given patient were correlated with each other for versican ($r^2 = 0.66$, $P = 0.003$) and CCL2 ($r^2 = 0.51$, $P = 0.004$).

Capacity of CCL2 to bind chondroitin sulfate chains

Versican's negatively charged CS chains can bind to chemokines such as CCL2, CCL3, and CCL5 via ionic interactions, and can function as a chemokine reservoir [28,29]. The versican isoforms V0 and V1, which were both elevated in SSc monocytes, have numerous CS chains attached to the GAG-binding domain and thus have a large capacity for binding chemokines [28]. Both versican and CCL2 are upregulated in SSc monocytes; to determine whether these form a complex, we examined CCL2's binding capacity using plastic plates coated with or without synthetic CS (Figure 6A). As expected, CCL2 was able to bind to the plates only when CS was present. Immunocytostaining showed the cellular localization of versican and CCL2 in the Golgi apparatus of monocytes; the representative images of SSc monocytes in Figure 6B show versican and CCL2 colocalized in the Golgi apparatus. Additional experiments using monocytes derived from a patient with SSc and a healthy control subject produced concordant findings. Since the Golgi plays an important role in the synthesis of proteoglycans [30], these results suggest that versican forms a complex with CCL2 before secretion by monocytes.

Chondroitin sulfate chains enhance CCL2-mediated monocyte migration

The chemokine CCL2 induces monocytes, neutrophils, and lymphocytes to migrate [31]. To examine whether CCL2's capacity to induce migration is enhanced by binding to versican's CS chains, we performed migration assays in a TransWell® double-chamber system using $CD14^+$ monocytes derived from healthy controls and SSc patients. First, monocytes were cultured in the upper chamber, and the lower chamber was pre-coated with CS or vehicle alone in the presence or absence of CCL2 (Figure 7A,B). Monocyte migration was promoted only in the presence of CS-coated plates treated with CCL2, and the strength of the effect depended on the CS concentration in the coating (Figure 7C,D). This enhanced monocyte migration was completely blocked by adding an anti-CCL2 neutralizing antibody (Figure 7E,F). Monocytes derived from a healthy control and an SSc patient showed the similar behavior. Concordant results were obtained in additional experiments using monocytes derived from three healthy controls and three SSc patients. These findings indicate that CCL2 activity is augmented by binding to CS chains.

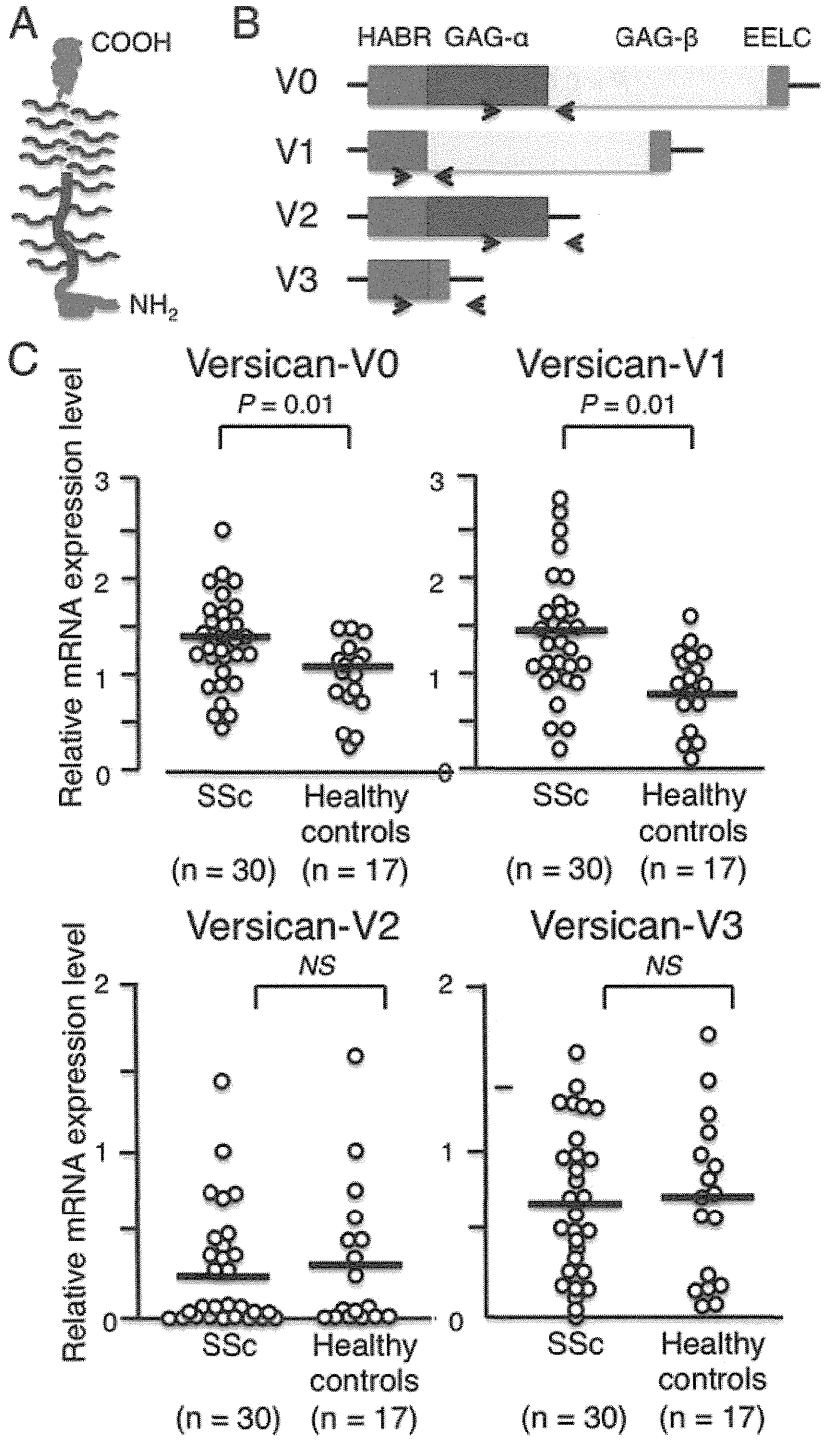

Figure 3 Versican splice variants and mRNA levels in monocytes from systemic sclerosis patients and healthy controls. **(A)** Molecular structure of full-length versican (V0), which has numerous chondroitin sulfate (CS) chains attached to its glycosaminoglycan (GAG)-binding domain. **(B)** mRNA structures of versican splice variants (V0, V1, V2 and V3). Versican is composed of a hyaluronan binding region (HABR, green), GAG-binding domains (blue and yellow), and epidermal growth factor-like, lectin-like, and complement-regulatory-like domains (EELC, red). Individual mRNA components are shown in the same color as their corresponding protein structures. Arrows denote primers used to amplify each splice variant. **(C)** Levels of versican V0, V1, V2, and V3 mRNA in systemic sclerosis (SSc) and control monocytes, analyzed using semi-quantitative PCR. Relative mRNA levels were calculated as a ratio of the expression level of the gene of interest to that of glyceraldehyde-3-phosphate dehydrogenase (GAPDH). Each bar in the graph denotes the mean. Differences between the two groups were analyzed by Mann-Whitney *U* test. NS, not significant.

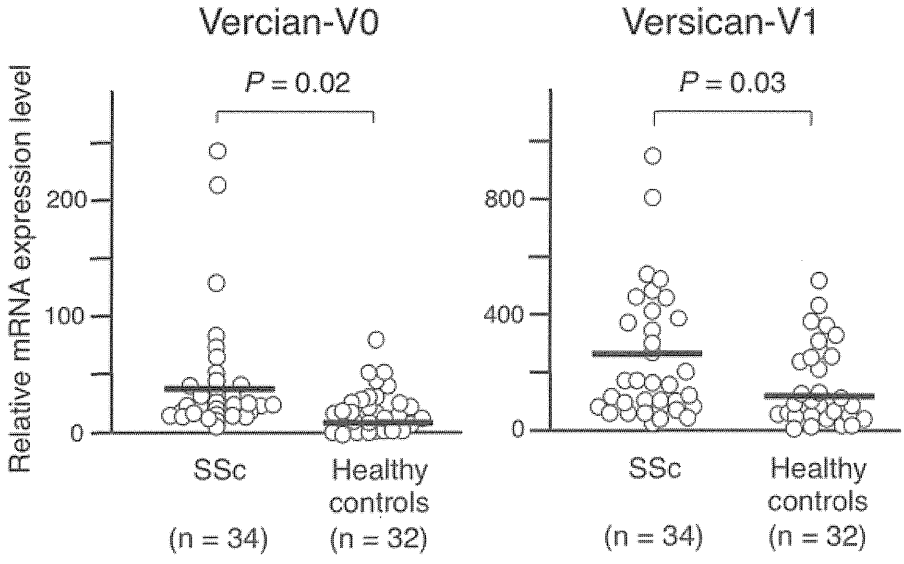

Figure 4 Versican V0 and V1 mRNA levels in systemic sclerosis and control monocytes. Quantitative PCR analysis. Relative mRNA levels were calculated as a ratio of the level of the gene of interest to that of glyceraldehyde-3-phosphate dehydrogenase (GAPDH). Each bar in the graph denotes the mean. Differences between the groups were analyzed by Mann-Whitney *U* test. SSc, systemic sclerosis.

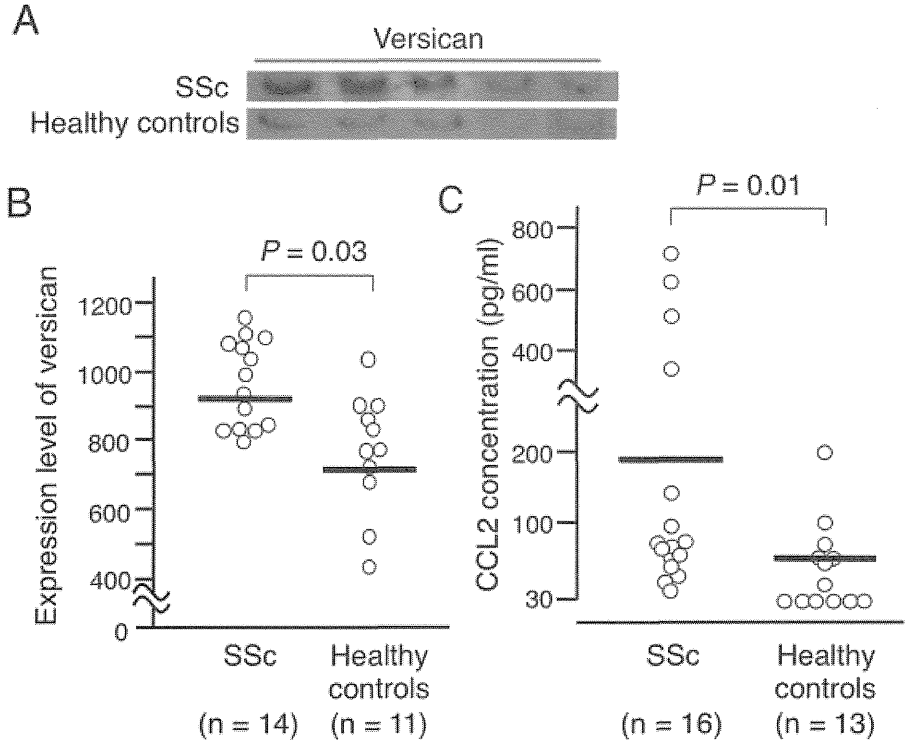

Figure 5 Versican V0 and CCL2 protein levels in monocyte culture supernatants. Versican V0 and CCL2 protein levels in monocyte culture supernatants derived from systemic sclerosis (SSc) patients and healthy controls. **(A)** Representative immunoblot evaluating versican V0 protein expression. Monocyte culture supernatants were concentrated, truncated, and applied to immunoblots. **(B)** Versican V0 protein levels in monocytes from 14 patients with SSc and 11 healthy controls, semiquantitatively measured by densitometry. **(C)** CCL2 protein levels in monocytes from 16 patients with SSc and 13 healthy controls. CCL concentration in culture supernatants was measured by an ELISA. Each bar in the graph denotes the mean. Results from the two groups were compared by Mann-Whitney *U* test.

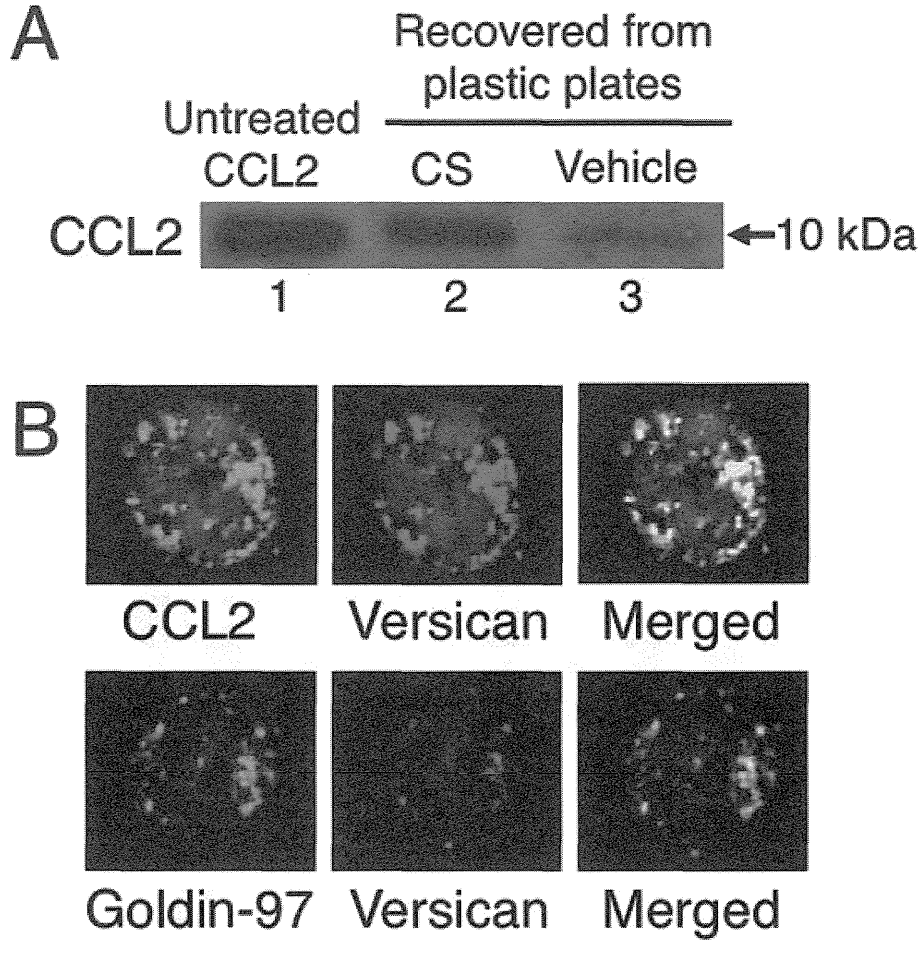

Figure 6 Formation of CCL2 and versican complex in circulating monocytes. **(A)** CCL2 was incubated with plastic plates coated with chondroitin sulfate (CS) or vehicle. Bound CCL2 was recovered and subjected to immunoblots (lanes 2 and 3, respectively). Lane 1, untreated CCL2 as a positive control. A representative result from three experiments is shown. **(B)** Versican and CCL2 cellular localization in monocytes from an systemic sclerosis (SSc) patient, assessed by multi-color immunocytostaining: upper panel, CCL2 (green), versican (red), and their merged image; lower panel, goldin-97 (green), versican (red), and their merged image. Nuclei were counterstained with TO-PRO3 (blue). A representative result from three independent experiments is shown. Original magnification, ×600.

Enhanced CCL2-mediated monocyte migration was probably due to the efficient formation of a chemotactic gradient, but it was also possible that CCL2 was protected from degradation when bound to a CS chain. To test this hypothesis, CCL2 was incubated with plates treated with CS or vehicle, and exposed to a variety of proteases that included elastase, cathepsin G, and trypsin. As shown in Figure 8A, CCL2 was degraded in the presence of proteases, but was protected from protease-mediated degradation when bound to the CS-coated plates. Concordant findings were obtained from three healthy controls (Figure 8B).

Discussion

This study has demonstrated that versican and CCL2 are upregulated in circulating $CD14^+$ monocytes in a subset of SSc patients. High versican levels in circulating monocytes were associated with fibrotic characteristics of SSc, such as diffuse cutaneous involvement. Interestingly, versican forms a reservoir for various CC chemokines that induce the migration of circulating monocytes, which produce additional versican after arriving at the versican-rich site. CCL2's ability to induce monocytes to migrate is enhanced by its binding to versican, due to the efficient formation of chemokine gradients and protection from proteolytic degradation. This positive feedback loop, consisting of versican, CCL2, and the influx of monocytes, may be enhanced at the affected sites of a subset of SSc patients with phenotypically altered circulating monocytes.

Versican is involved in many physiologic and pathologic processes, including neuronal development [32], atherosclerosis [33], and the invasive and metastatic

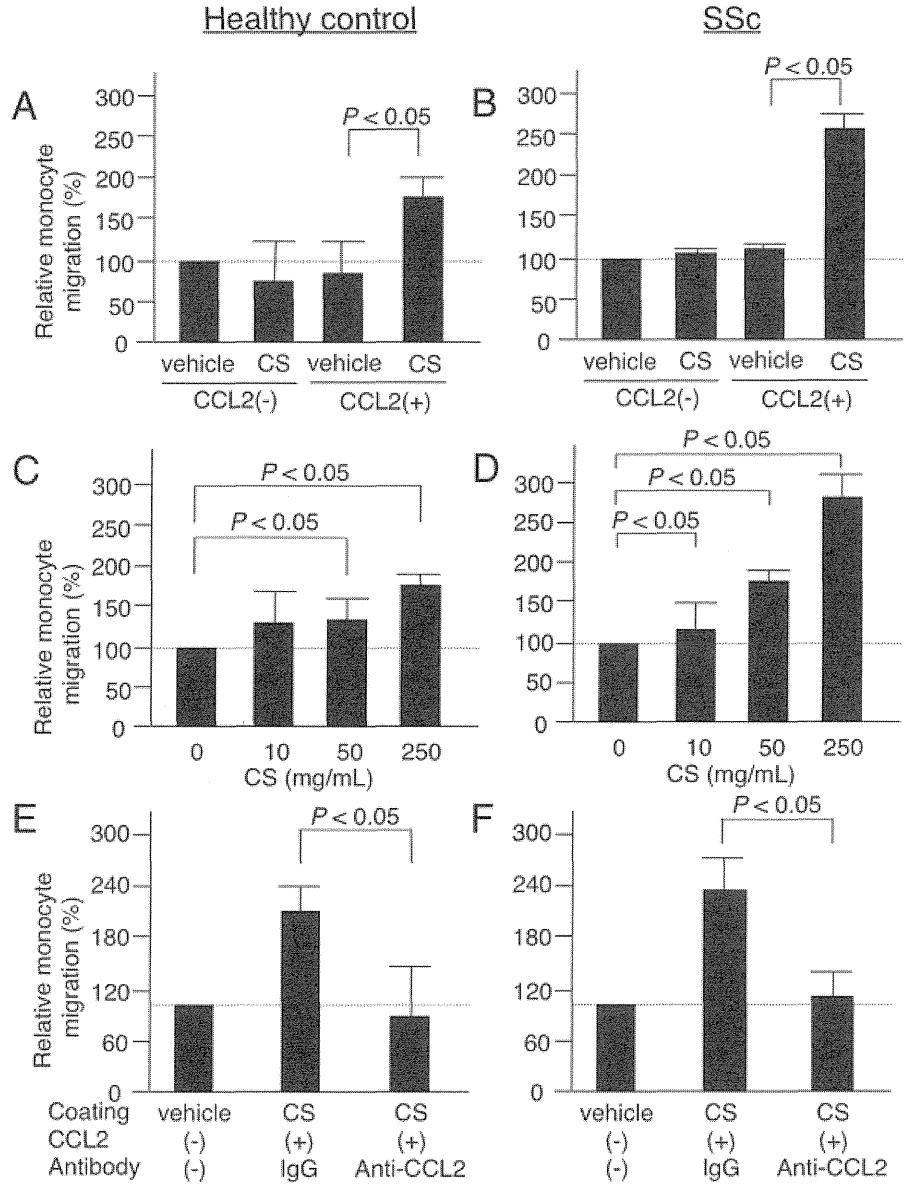

Figure 7 CCL2 chemoattractant activity promoting monocyte migration, with or without chondroitin sulfate binding. Circulating monocytes derived from healthy controls (A, C, E) and systemic sclerosis (SSc) patients (B, D, F). **(A, B)** CCL2-induced monocyte migration in the presence or absence of chondroitin sulfate (CS) coating. Lower chambers of a TransWell® double-chamber system (Corning Incorporated, Corning, NY, USA) were coated with CS or vehicle, and $CD14^+$ monocytes were applied to the upper chambers. **(C, D)** CCL2-induced monocyte migration on plastic plates precoated with serial concentrations of CS. **(E, F)** CCL2-induced monocyte migration on CS-coated plastic plates in the presence of anti-CCL2 mAb or control IgG. Relative monocyte migration was calculated as a percentage of migration in a control experiment using vehicle-coated wells without CCL2. All experiments were carried out in duplicate; the mean and standard deviation of three measurements is shown. Results from the two groups were compared using a Mann-Whitney *U* test. A representative result from four independent experiments is shown.

signatures of many cancers [34]. As with other ECM components, versican is enriched in the skin of patients with SSc [35], although little is known about versican's role in SSc pathogenesis. Versican is able to bind type I collagen and hyaluronic acid to maintain the integrity of the ECM [28], which may be important in forming the stiff fibrotic tissue seen with SSc. Versican also functions as a unique reservoir for a variety of growth factors, chemokines, and cytokines, which it gathers via numerous CS chains attached to its GAG-binding domain [28]. Chemokines known to bind versican include CCL2, CCL3, CCL5, CCL21, CXCL10, and CXCL12. It is